Generation and characterization of HIV-1 clones chimeric for subtypes B and C *nef*

ABHAY JERE[1,2], AHMAD PIROOZMAND[1], SRIKANTH TRIPATHY[2], RAMESH PARANJAPE[2],
AKIKO SAKURAI[1], MIKAKO FUJITA[1] and AKIO ADACHI[1]

[1]Institute of Health Biosciences, The University of Tokushima Graduate School,
Tokushima 770-8503, Japan; [2]National AIDS Research Institute (NARI), Pune 411026, India

Abstract. The impact of human immunodeficiency virus type 1 (HIV-1) Nef on viral infectivity was evaluated by characterization of chimeric clones. Chimera with respect to the *nef* gene were constructed between subtypes B and C, and monitored for their replication in human peripheral blood mononuclear cells. The parental clones used were pNL432 (subtype B) and pIndie-C1 (Indian subtype C), which show considerable sequence heterogeneity in *nef* and distinct viral growth phenotype. While an enhancing effect of Nef on viral infectivity was noted, no significant growth difference was observed between the parental and chimeric clones. The difference in growth potential of the two subtype clones was mainly ascribable to viral sequence(s) other than *nef*. Our results here clearly showed that HIV-1 Nef does not significantly affect the *in vitro* viral infectivity in natural target cells.

Introduction

Human immunodeficiency virus type 1 (HIV-1) subtype C is currently predominating HIV global pandemic. More than 56% of all HIV-1 infections are attributed to subtype C. Epidemiological studies have revealed the presence of subtype C virus in divergent regions of world such as India, China and parts of the African continent (1). Over 4 million Indians are estimated to be HIV-1-infected and >80% of the strains belong to subtype C (2). Phylogenetic sequence analysis of *gag* and *env* has shown that Indian sequences segregate apart from other subtype C sequences suggesting a subclade within subtype C (3). Recently, we also reported a similar observation for accessory gene *nef* from a large number of Indian samples (4).

Many reports are available discussing subtype specific sequence variability for various HIV-1 genes. But to date, no data have been published that directly correlate the sequence polymorphism to alterations in virological properties. Extensive functional studies on HIV-1 subtype B have been carried out (5), but they may not be directly correlated to subtype C virus due to large sequence variability (6). Functional studies focused on subtype C or Indian subtype C virus are scarce (7).

Our present study aimed at a functional comparison of HIV-1 accessory protein Nef from subtypes B and C for its ability to confer infectivity on virions. The critical role of *nef* in AIDS pathogenesis was first emphasized with an observation that some subjects infected with the virus carrying naturally-occurring *nef* deletions became long-term non-progressors (8,9). Nef is a 25-30 kD early protein believed to be crucial for viral replication. Multiple functions have been attributed to Nef, such as down-regulation of cell surface CD4 and MHC-I molecules, modulation of cellular activation and role in controlling apoptosis of infected cells, thus making Nef one of the most enigmatic proteins of HIV (10,11). More than 30 putative Nef functions and targets have been identified, but the detailed molecular mechanisms underlying these effects are still unclear (12). In this study, we established a cloning system that facilitated the exchange of *nef* from pNL432 (subtype B) (13) and pIndie-C1 (Indian subtype C) (14). Reporter B/C and C/B chimeric clones for *nef* were constructed and examined for their *in vitro* infectivity in human peripheral blood mononuclear cells (PBMCs).

Materials and methods

Cells. Human PBMCs were separated from buffy coats obtained from healthy donors and cultured as previously described (15). A monolayer cell line 293T (16) was maintained in Eagles's minimal essential medium containing 10% heat-inactivated fetal bovine serum as previously described (13).

Transfection and reverse transcriptase (RT) assay. Uncleaved plasmid DNA was introduced to 293T cells by the calcium-phosphate co-precipitation method as described before (13). RT assay using ^{32}P-dTTP has been previously described (17).

Correspondence to: Dr Akio Adachi, Department of Virology, Institute of Health Biosciences, The University of Tokushima Graduate School, Tokushima 770-8503, Japan
E-mail: adachi@basic.med.tokushima-u.ac.jp

```
                          polymorphic region
                myristoylation         ↓        variable region                    proteolytic cleavage

NL432    1  MGGKWSKSSVIGWPAVRERMRRAEPAADGVGAVSRDLEKHGAITSSNTAANNAACAWLEA  60
IndieC   1  MGGKWSKCSIVGWPAIRERMRRAEPAAEGVGAASQDLDKHGALTSSNTDTTNADCAWLRA  60
            ******* *  ****  *********** ****  *  **  ****  *****    **  **** *

                        (Pro-X-X-Pro)₃
              acidic region        ↓                                      basic residue

NL432   61  QEEE-EVGFPVTPQVPLRPMTYKAAVDLSHFLKEKGGLEGLIHSQRRQDILDLWIYHTQG  119
IndieC  61  QEEEGEVGFPVTPQVPLRPMTYKSAFDLSFFLKEKGGLEGLIYSKKRQEILDLWVYHTQG  120
            ****  *****************  *  *  ***  ************  *   **  *****  *****

                                    Pro-X-X-Pro        Dileucine motif

NL432  120  YFPDWQNYTPGPGVRYPLTFGWCYKLVPVEPDKVEEANKGENTSLLHPVSLHGMDDPERE  179
IndieC 121  FFPDWQNYTPGPGVRYPLTFGWCFKLVPVDPREVEEANEGEDNCLLHPVCQHGMEDEHRE  180
            ********************* ****  *   *****  **   *****  ***  *   **

NL432  180  VLEWRFDSRLAFHHVARELHPEYFKNC  206
IndieC 161  VLKWKFDSQLARRHMARELHPEFYKDC  207
            **  *  *** **   *  *******   * *
```

Figure 1. Amino acid sequence alignment for HIV-1 Nef from NL432 (subtype B) and Indie-C1 (Indian subtype C). Amino acid sequences are obtained from GenBank (accession nos. AF324493 and AB023804 for NL432 and Indie-C1, respectively), and aligned by the ClustalW 1.8 sequence alignment program (4). Important functional domains are indicated (4). Conserved amino acids are shown by *. IndieC, Indie-C1.

Figure 2. Schematic representation of various proviral clones used in this study. Structures of parental (NL/nCM and Indie/nCM), chimeric (NL/n-Ind and Indie/n-NL), and *nef*-deficient (NL/nCM-Xh and Indie/nCM-Xh) clones are shown. NL and Indie sequences are indicated by white and grey boxes, respectively. Open and closed triangles represent *Cla*I and *Mlu*I sites, respectively. The original clones pNL432 (NL432) and pIndie-C1 (IndieC) are also shown. LTR, long terminal repeat.

Western immunoblotting. Cell lysates were prepared as described before (17), and proteins were resolved on sodium dodecyl sulfate-12.5% polyacrylamide gels, followed by electrophoretic transfer to polyvinylidene fluoride membranes (Immobilon-P, Millipore, Bedford, MA, USA). The membranes were treated with anti-Nef antiserum provided by Dr Swanstrom (through the AIDS Research and Reference Reagent Program, Division of AIDS, National Institute of Infectious Diseases (NIAIDS), National Institutes of Health (NIH) and anti-Gag-p24 antibody (18), and visualized by ECL plus the Western blotting detection system (Amersham Pharmacia Biotech Inc., Buckinghamshire, UK) (19).

Infection of human PBMCs. Infection of human PBMCs was initiated in 24-well plates by incubating 1×10^6 cells per sample for 18 h with viral supernatants that were normalized to 10^5 RT units of cell-free virus. Input virus was then removed, and cells were cultured in 1 ml of standard growth medium for PBMCs. Culture supernatants were harvested every 3 days, and stored at -80°C until RT activity was determined.

A
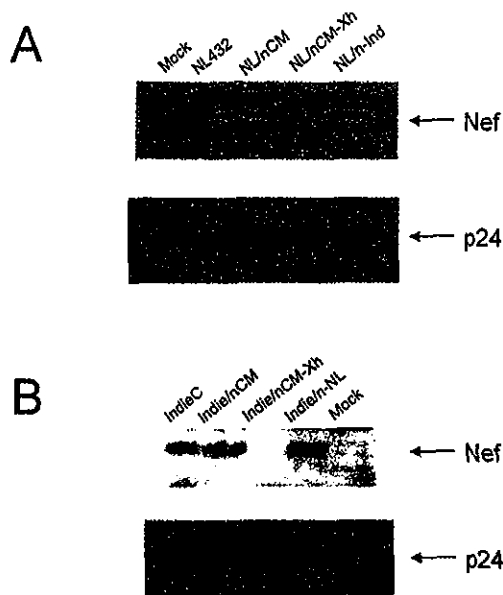

← Nef

← p24

B

← Nef

← p24

Figure 3. Monitoring the expression of Nef and Gag-p24 in transfected 293T cells. The 293T cells were transfected with various clones indicated, and cell lysates for Western blot analysis using appropriate antibodies were prepared on day 2 post-transfection. Results are shown separately for NL-derived (A) and Indie-derived (B) clones. Mock, pUC 19; IndieC, Indie-C1.

Sequence alignment. Amino acid sequences of pNL432 Nef (GenBank accession no. AF324493) and pIndie-C1 Nef (GenBank accession no. AB023804) were aligned (Fig. 1) using ClustalW 1.8 sequence alignment program (4).

DNA constructs. Infectious proviral clones of HIV-1 designated pNL432 (subtype B) (13) and pIndie-C1 (Indian subtype C) (14,20) were used as parental clones. Appropriate fragments of pNL432 and pIndie-C1 were subcloned into pBluescript SK(+) (Stratagene, La Jolla, CA, USA). On subcloning, ClaI

and MluI restriction enzyme sites were introduced at 5' and 3' ends of *nef*, respectively, using the QuickChange site-directed mutagenesis kit (Stratagene). The mutated fragments were cloned back into pNL432 and pIndie-C1 to construct basic clones pNL/nCM and pIndieC/nCM (Fig. 2). The *nef* genes of these clones were then exchanged to construct chimeric pNL/n-Ind (pNL432 containing *nef* from pIndie-C1) and pIndie/n-NL (pIndie-C1 containing *nef* from pNL432) (Fig. 2). Clone pNL/nCM-Xh (NL/ΔNef) was also constructed by introducing a frame-shift mutation at the *Xho*I site present at N-terminal region of NL432 *nef* (Fig. 2). The mutated *nef* of pNL/nCM-Xh was used to construct pIndie/nCM-Xh (Indie/ΔNef) (Fig. 2).

Results and Discussion

We recently reported that sequence variability in Nef between subtype B and Indian subtype C viruses ranges from 15 to 25% (4). Variability is predicted to be a result of either evolutionary pressure giving the virus an advantage for survival (non-synonymous substitutions) or silent, harmless synonymous substitutions along the course of evolution. To determine the biological and functional significance of this naturally-occurring sequence variability, we constructed chimeric clones with respect to *nef* using infectious pNL432 (subtype B) (13) and pIndie-C1 (Indian subtype C) proviral clones (14) with distinct virological properties (20). By monitoring and comparing the infectivity of *nef*-chimeric clones in human PBMCs, the functional importance of Nef in natural target cells would be readily evaluated.

Fig. 1 shows the sequence alignment for Nef proteins of NL432 and Indie-C1. While important functional domains are well-conserved, some variations are observed in juxtapositions to these crucial regions and hence may influence the functionality of Nef (4). To ensure the construction of *nef*-chimeric clones, ClaI and MluI restriction enzyme sites
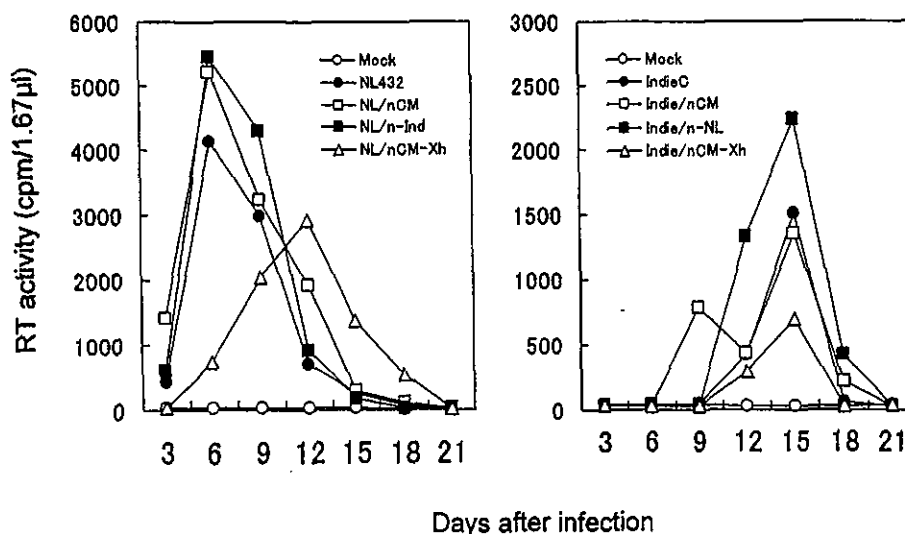

Days after infection

Figure 4. Growth kinetics in human PBMCs of various viruses. Input virus samples were obtained from 293T cells transfected with various proviral clones indicated (see Fig. 2). Human PBMCs stimulated with PHA-P (10^6 cells) were infected with an equal amount of virus (10^5 RT units), and virus replication was monitored at intervals by RT production in the culture supernatants. Results are separately shown for NL-derived (left) and Indie-derived (right) viruses. Mock, pUC19; IndieC, Indie-C1.

were introduced into the 5' and 3' ends of *nef* in pNL432 and pIndie-C1 (Fig. 2). To ascertain the Nef-dependency of viral infectivity in PBMCs, frame-shift *nef*-deficient mutants designated pNL/nCM-Xh and pIndie/nCM-Xh were constructed. Various clones thus constructed (Fig. 2) were monitored for the expression of Nef and Gag-p24 (as control) in cells. The 293T cells were transfected with the clones, and 2 days later, cell lysates were prepared for Western blot analysis. As shown in Fig. 3, Nef was readily detected in transfected cells except for control samples (ΔNef mutants and mock).

Infectivity of various proviral clones (Fig. 2) were then determined in human PBMCs. Input virus samples were prepared from 293T cells transfected with the clones, and inoculated into freshly-isolated human PBMCs. Fig. 4 shows the growth kinetics of viruses obtained. *Nef*-positive parental and its chimeric clones grew quite similarly (NL- and Indie-derived clones in left and right panels, respectively). The negative effect of Nef-deficiency on virus replication was obvious for viruses with NL (left) or Indie (right) background. When the growth rates of various viruses were compared, it was found that NL-viruses grew much better than Indie-viruses. RT production reached a peak on day 6 post-infection for NL-viruses (left), and on day 15 for Indie-viruses (right). Our data in Fig. 4 showed that while Nef can enhance viral infectivity somewhat, a distinct viral factor(s) other than Nef contributes much to the *in vitro* infectivity in natural target PBMCs. Previously, we reported that there is no clear correlation between *nef*-deletions and long-term non-progression of HIV-1 infection (4). These findings compositely suggest that Nef solely may not significantly influence the *in vivo* viral infectivity nor pathogenicity.

As the HIV-1 epidemic has progressed, there is strong emergence of subtype C infections, and subtype C viruses are currently predominant worldwide. One of the reasons responsible for this could be the unique biological property of subtype C virus. Although we demonstrated a significant growth difference between subtype B NL432 and subtype C Indie-C1 (Fig. 4), it is unclear how subtype C in general is biologically different from the other subtypes. Because Indie-C1 is the only subtype C-infectious clone available to date, more infectious clones in this group need to be constructed and carefully investigated. Our system, as described in this report, can thus be used to address this critical issue.

Acknowledgements

References

1. Ball SC, Abraha A, Collins KR, Marozsan AJ, Baird H, Quinones-Mateu ME, Penn-Nicholson A, Murray M, Richard N, Lobritz M, Zimmerman PA, Kawamura T, Blauvelt A and Arts EJ: Comparing the *ex vivo* fitness of CCR5-tropic human immunodeficiency virus type 1 isolates of subtypes B and C. J Virol 77: 1021-1038, 2003.
2. Lole KS, Bollinger RC, Paranjape RS, Gadkari D, Kulkarni SS, Novak NG, Ingersoll R, Sheppard HW and Ray SC: Full-length human immunodeficiency virus type 1 genomes from subtype C-infected seroconverters in India, with evidence of intersubtype recombination. J Virol 73: 152-160, 1999.
3. Gaschen B, Taylor J, Yusim K, Foley B, Gao F, Lang D, Novitsky V, Haynes B, Hahn BH, Bhattacharya T and Korber B: Diversity considerations in HIV-1 vaccine selection. Science 28: 2354-2360, 2002.
4. Jere A, Tripathy S, Agnihotri K, Jadhav S and Paranjape R. Genetic analysis of Indian HIV-1 nef: subtyping, variability and implications. Microbes Infect 6: 279-289, 2004.
5. Freed EO and Martin MA: HIVs and their replication. In: Virology. Knipe DM, Howley PM, Griffin DE, Martin MA, Lamb RA, Roizman B and Straus SE (eds). Lippincott Williams & Wilkins, Philadelphia, pp1971-2041, 2001.
6. Paranjape RS, Gadkari DA, Lubaki M, Quinn TC and Bollinger RC: Cross-reactive HIV-1-specific CTL in recent sero-converters from Pune, India. Indian J Med Res 108: 35-41, 1998.
7. Cecilia D, Kulkarni SS, Tripathy SP, Gangakhedkar RR, Paranjape RS and Gadkari DA: Absence of coreceptor switch with disease progression in human immunodeficiency virus infections in India. Virology 5: 253-258, 2000.
8. Dyer WB, Geczy AF, Kent SJ, McIntyre LB, Blasdall SA, Learmont JC and Sullivan JS: Lymphoproliferative immune function in the Sydney Blood Bank Cohort, infected with natural nef/long terminal repeat mutants, and in other long-term survivors of transfusion-acquired HIV-1 infection. AIDS 11: 1565-1574, 1997.
9. Kirchhoff F, Greenough TC, Brettler DB, Sullivan JL and Desrosiers RC: Brief report: absence of intact nef sequences in a long-term survivor with nonprogressive HIV-1 infection. N Eng J Med 26: 228-232, 1995.
10. Arold ST and Baur AS: Dynamic Nef and Nef dynamics: how structure could explain the complex activities of this small HIV protein. Trends Biochem Sci 26: 356-363, 2001.
11. Geyer M, Fackler OT and Peterlin BM: Structure-function relationships in HIV-1 Nef. EMBO Rep 2: 580-585, 2001.
12. Fackler OT and Baur AS: Live and let die: Nef functions beyond HIV replication. Immunity 16: 493-497, 2002.
13. Adachi A, Gendelman HE, Koenig S, Folks T, Willey R, Rabson A and Martin MA: Production of acquired immuno-deficiency syndrome-associated retrovirus in human and nonhuman cells transfected with an infectious molecular clone. J Virol 59: 284-291, 1986.
14. Mochizuki N, Otsuka N, Matsuo K, Shiino T, Kojima A, Kurata T, Sakai K, Yamamoto N, Isomura S, Dhole TN, Takebe Y, Matsuda M and Tatsumi M: An infectious DNA clone of HIV type 1 subtype C. AIDS Res Hum Retroviruses 20: 1321-1324, 1999.
15. Tokunaga K, Ishimoto A, Ikuta K and Adachi A: Growth ability of auxiliary gene mutants of human immunodeficiency virus types 1 and 2 in unstimulated peripheral blood mononuclear cells. Arch Virol 142: 177-181, 1997.
16. Lebkowski JS, Clancy S and Calos MP: Simian virus 40 replication in adenovirus-transformed human cells antagonizes gene expression. Nature 12: 169-171, 1985.
17. Willey RL, Smith DH, Lasky LA, Theodore TS, Earl PL, Moss B, Capon DJ and Martin MA: *In vitro* mutagenesis identifies a region within the envelope gene of the human immunodeficiency virus that is critical for infectivity. J Virol 62: 139-147, 1988.
18. Akari H, Fukumori T and Adachi A: Cell-dependent requirement of human immunodeficiency virus type 1 gp41 cytoplasmic tail for Env incorporation into virions. J Virol 74: 4891-4893, 2000.
19. Fujita M, Akari H, Sakurai A, Yoshida A, Chiba T, Tanaka K, Strebel K and Adachi A: Expression of HIV-1 accessory protein Vif is controlled uniquely to be low and optimal by proteasome-degradation. Microbes Infect (In press).
20. Tobiume M, Takahoko M, Tatsumi M and Matsuda M: Establishment of a MAGI-derived indicator cell line that detects the Nef enhancement of HIV-1 infectivity with high sensitivity. J Virol Methods 97: 151-158, 2001.

Differential modulation of gene expression among rat tissues with warm ischemia

Yukiko Miyatake[a], Hitoshi Ikeda[a], Rie Michimata[a,b], Seiko Koizumi[a], Akihiro Ishizu[a], Norihiro Nishimura[b], Takashi Yoshiki[a,b,*]

[a]Department of Pathology/Pathophysiology, Division of Pathophysiological Science, Hokkaido University Graduate School of Medicine, Sapporo 060-8638, Japan
[b]Genetic Lab, Sapporo 060-0009, Japan

Abstract

The aim of this study is to determine if warm ischemia after surgical extirpation impacts gene expression in tissue samples which will be used for cDNA array analysis. We investigated effects of warm ischemia on gene expression in lung, liver, kidney, and spleen of rats, chronologically, using an original cDNA array, real-time quantitative RT-PCR and immunohistochemistry. Although no visible alteration was found in RNA quality, cDNA array showed that expression of many genes was modulated by warm ischemia within 60 min in these tissues, 19.1% of the tested genes in lung, 11.0% in liver, 5.1% in kidney, and 16.2% in spleen. Quantitative RT-PCR revealed that warm ischemia significantly induced up-regulation of immediate early genes, c-fos, Egr-1, and c-jun, in lung, but not in liver. These findings suggest that genes may show tissue-dependent differential transcriptional response against warm ischemia. Tissue samples obtained from patients during surgery cannot completely escape effects of ischemia. In case of examination by cDNA array analysis, biologists should keep in mind that tissue samples come equipped with particular footprints.
© 2004 Elsevier Inc. All rights reserved.

Keywords: Warm ischemia; Differential modulation; Gene expression; Immediate early genes; cDNA array; c-fos; Egr-1; c-jun

Introduction

cDNA array techniques have made feasible to monitor the comprehensive expression of numerous genes. The technique has been applied to not only in vitro and in vivo experiments in basic medical research using culture cells and animal models but also to clinical research using extirpated tissues from patients with various disorders. These data are used for diagnostic indicators, prognostic markers, selection and assignment of chemotherapy, and monitoring desired or adverse outcomes of therapeutic interventions that may direct individualized clinical management (Bertucci et al., 2003; Bunney et al., 2003; Gerhold et al., 2002). Ischemia–reperfusion injury associated with surgical extirpation of tissues has significant effects on gene expression (Brand et al., 2003; Goto et al., 1994; Itoh et al., 2000; Plumier et al., 1996; Sakai et al., 2003). Recently, cDNA array revealed that mRNAs isolated from tissues extirpated surgically under different conditions, such as ischemic time at operations and passage of time from excision until flash freezing for fixation, might include modulations on gene expression caused not only by genetic alternations in particular diseases but also effects related to conditions when samples were obtained (Dash et al., 2002; Huang et al., 2001). To avoid artificial modulations of gene

* Corresponding author. Department of Pathology/Pathophysiology, Division of Pathophysiological Science, Hokkaido University Graduate School of Medicine, Kita-15, Nishi-7, Kita-ku, Sapporo 060-8638, Japan. Fax: +81 11 706 7825.
E-mail address: path1@med.hokudai.ac.jp (T. Yoshiki).

expression caused by warm ischemia, tissue samples for mRNA isolation must be extracted as rapidly as possible. Although this procedure is feasible for cultured cells and small animal models, it is not always practicable for surgical tissue samples from humans. Therefore, researchers must be aware that alternations of gene expression in surgical tissue materials can occur by artificial effects such as warm ischemia; otherwise, spread of cDNA array techniques could yield questionable vast data on gene expression changes.

In the present study, we investigated effects of warm ischemia on gene expression in lung, liver, kidney, and spleen of rats, chronologically, using an original cDNA array filter equipped with 271 genes related to apoptosis, cell cycle regulation, and signal transduction. Using the real-time reverse transcriptase-polymerase chain reaction (RT-PCR) and immunohistochemistry, we confirmed the mRNA expression and protein production concerning some genes quantitatively.

Materials and methods

Preparation of rat cDNA array filter

To spot cDNA probes for rat genes on an original array filter, partial cDNAs of 271 rat genes were cloned. Briefly, total RNAs were isolated from various tissues of several rat strains, using ISOGEN reagent (Nippon Gene Co. Ltd., Toyama, Japan), and were reverse-transcribed, using Moloney murine leukemia virus (M-MLV) RT (Invitrogen Co., Carlsbad, CA) and oligo(dT) (Invitrogen) or random primers (TAKARA Shuzo Co., Kyoto, Japan). Using the synthesized cDNAs as a template, approximately 500 bp of fragments were PCR amplified, using TAKARA Ex Taq™ polymerase (TAKARA) and specific synthetic primers for rat genes. Sequence information was obtained from the National Center for Biotechnology Information (NCBI, MD, USA). Human or mouse sequences were also used in primer synthesis when adequate information for rat gene sequences was not available. Amplified fragments were ligated into PGEM®-T Easy-Vector (Promega, Madison, WI, USA) and the sequences were confirmed to be correct by DNA sequencing, using ABI PRISM 310 Gene Analyzer (Applied Biosystems, Foster City, CA, USA). The identified cDNA fragments were re-amplified by 25 cycles of PCR using a standard vector primer set. Each amplified product was spotted in duplicate at 0.3 ng each on a nylon membrane filter, HYDRA96-HTS (Lab. Co. Ltd., Sapporo, Japan), according to manufacturer's protocols. After drying for overnight at room temperature, the membranes were treated with 0.5M NaOH/1.5M NaCl and rinsed with 0.5M Tris–HCL/1.5M NaCl for 5 min at room temperature, respectively, then dried and cross-linked at 125 mJ under an ultraviolet lamp.

Preparation of rat tissues with warm ischemia

Three male Wistar–King–Aptekman–Hokudai rats (350–450 g body weight), obtained from the Institution of Animal Experimentation, Hokkaido University Graduate School of Medicine, were anesthetized by giving intraperitoneal injection of sodium pentobarbital (75 mg/kg). Lung, kidney, spleen, and liver were extracted within 1 min, and then rapidly divided into four pieces of equal volume, respectively. One piece of each tissue was quickly flash-frozen in liquid nitrogen and used as a sample without ischemia (0 min), while the other three pieces of each tissue were maintained at room temperature (27°C). At 10, 30, or 60 min after extirpation, tissues were flash-frozen in liquid nitrogen and served as chronological samples affected by warm ischemia, respectively. All of samples were stored at −80°C until use.

Preparation of biotin labeled cDNA probes

Total RNAs of each tissue, with or without warm ischemia, were obtained using ISOGEN reagents and purified using an RNeasy® Mini Kit (Qiagen, Santa Clarita, CA, USA). After checking the quality, the total RNAs were treated with DNase I, and poly(A)$^+$mRNAs were purified using a mRNA Purification kit (MagExtractor®-mRNA-, TOYOBO Co. Ltd., Osaka, Japan). With the Gene Navigator® cDNA Amplification System ver.2 (TOYOBO Co. Ltd.), biotin-labeled cDNA probes were generated from the purified mRNAs. Briefly, 1 μg of each purified mRNA was reverse-transcribed using ReverTra Ace® and oligo(dT) primers with synthetic anchor sequences, and 3′-end of the cDNA was tailed to poly(dA) using dATPs and
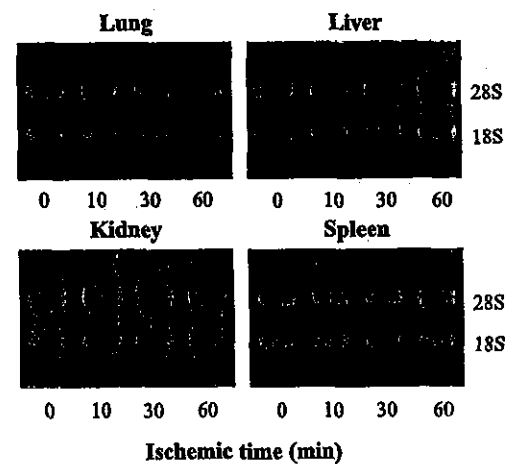

Fig. 1. Quality of total RNA in each sample with warm ischemia. The quality of total RNA was confirmed by 28S/18S ribosomal RNA ratio in the standard electrophoresis gel with ethidium bromide staining. No significant difference was evident among samples with or without warm ischemia within 60 min. Zero minute means sample without ischemia, and 10, 30, and 60 min mean time exposed to warm ischemia. Representative data for each organ in three rats are shown.

Table 1
List of genes affected by warm ischemia in each rat tissue examined

Up		Ischemic time (min)			Down		Ischemic time (min)		
Gen Bank ID	Gene name	10	30	60	Gen Bank ID	Gene name	10	30	60
Lung									
Genes reached maximum intensity at 10 min					Genes reached at 0.5-fold at 10 min				
NM_004530	MMP-2	7.2	3.3	4.4	NM_012752	CD24	0.5	0.8	1.0
NM_031761	VEGF-D	3.8	0.0	0.0	AF246634	IкB-β	0.5	0.7	1.2
NM_012922	Caspase-3	3.5	0.0	0.0	U22520	IP10	0.5	0.4	0.7
X54419	IL-5	3.4	0.0	0.7	AF177757	ING1	0.4	1.5	1.8
NM_021850	Bcl-W	3.3	0.5	1.7	NM_012923	cyclin G1	0.3	0.7	1.0
U72353	Lamin B1	3.1	1.3	2.7	NM_017064	STAT5 alpha	0.2	0.6	0.5
NM_012842	EGF	2.7	0.0	0.0	NM_133293	GATA-3	0.2	0.1	0.7
NM_016787	Nip2	2.5	0.5	0.0	AF055292	STAT6	0.0	0.7	0.5
NM_023979	Apaf-1	2.5	0.6	0.0	NM_010786	MDM2	0.0	0.0	0.9
NM_013091	TNFR1	2.3	0.7	0.9	NM_007635	cyclin G2	0.0	0.0	0.0
NM_011234	RAD51	2.1	1.3	0.0	NM_0125551	Ets-1	0.0	0.0	0.0
Genes reached maximum intensity at 30 min					S73518	FGFR-1	0.0	0.0	0.0
NM_010817	pSMD7	3.1	3.4	2.6	Genes reached at 0.5-fold at 30 min				
NM_031535	Bcl-XL	1.9	2.9	2.2	NM_031775	Caspase-6	1.0	0.5	0.8
U25995	RIP	1.9	2.3	0.0	NM_012789	CD26	0.8	0.5	0.0
XM_134721	p19ink4d	0.6	2.0	1.1	Z38067	c-myc	0.8	0.4	1.0
NM_010817	pSMD7	3.1	3.4	2.6	NM_019165	IL-18	1.2	0.4	1.0
NM_031535	Bcl-XL	1.9	2.9	2.2	NM_130860	Cdk9	1.0	0.4	1.0
U25995	RIP	1.9	2.3	0.0	X83579	Cdk7	0.6	0.3	0.6
XM_134721	p19ink4d	0.6	2.0	1.1	AF010466	Interferon-γ	1.0	0.0	0.0
Genes reached maximum intensity at 60 min					NM_012889	VCAM-1	0.8	0.0	0.0
X06769	c-fos	0.9	4.3	6.5	AF055291	STAT4	0.6	0.0	0.0
NM_012551	EGR-1	1.0	3.5	5.4	Genes reached at 0.5-fold at 60 min				
NM_012675	TNF-alpha	1.0	1.0	3.0	NM_012830	CD2	1.2	1.0	0.5
AJ441127	FADD	1.0	1.0	2.6	S40706	GADD153	1.2	0.7	0.5
D14014	cyclin D1	2.1	2.0	2.5	NM_031643	MEK-1	1.2	0.7	0.5
J00750	metallothionein-1	0.6	0.9	2.2	NM_012855	JAK3	0.6	0.8	0.4
NM_053743	Cdc37	1.2	1.4	2.1	NM_021846	Mcl-1	0.8	0.7	0.3
L09653	TGFβ-RII	0.5	0.1	2.1	AJ000556	JAK1	0.9	0.7	0.0
AY027667	Caspase-9	1.6	1.2	2.1					
NM_024388	NGF beta	0.8	0.7	2.0					
Liver									
Genes reached maximum intensity at 10 min					Genes reached at 0.5-fold at 10 min				
NM_017218	ErbB-3	4.0	3.5	2.7	AF055292	STAT6	0.4	0.5	0.0
NM_012789	CD26	2.9	2.4	2.4	X14879	RT-1Ba (MHC Class II)	0.3	0.0	0.0
NM_031775	Caspase-6	2.8	2.7	2.3					
AB015747	IL-4R	2.8	2.2	1.8					
AF235993	Bax	2.8	1.6	1.8					
M31018	RT-1Aa (MHC Class I)	2.7	2.5	2.6					
NM_012967	ICAM-1	2.7	2.1	1.9					
NM_022177	CXCR-4	2.5	2.3	2.3					
NM_012551	EGR-1	2.5	1.9	1.3					
NM_053593	Cdk4	2.4	2.3	2.1					
AY027667	Caspase-9	2.0	1.9	0.1					
X63594	IкB-α	2.0	1.8	1.5					
NM_010219	Immunophilin	2.0	1.7	1.7					
Genes reached maximum intensity at 30 min									
NM_053727	nuclear factor IL3 regulated	2.5	3.3	2.0					
NM_009736	Bag-1	2.3	3.0	1.5					
U37252	14-3-3 protein zetasubtype	2.1	2.9	2.0					
L37092	p130 PITSL	2.6	2.8	1.5					
AF177757	ING1	1.3	2.8	1.6					
AK018592	TRADD	1.6	2.4	0.4					
NM_130860	Cdk9	1.6	2.3	1.3					
AF246634	IкB-β	1.9	2.1	1.9					
XM_125724	Cdc34	1.8	2.1	1.7					
X62853	Grb2	1.3	2.1	1.5					

Table 1 (*continued*)

Up					Down				
Gen Bank ID	Gene name	Ischemic time (min)			Gen Bank ID	Gene name	Ischemic time (min)		
		10	30	60			10	30	60
Liver									
NM_080885	Cdk5	1.6	2.0	1.1					
NM_010817	pSMD7	1.7	2.0	1.3					
Genes reached maximum intensity at 60 min									
NM_013091	TNFR1	1.7	3.0	3.6					
NM_053743	Cdc37	2.3	2.0	2.5					
J00750	metallothionein-1	1.8	1.8	2.0					
Kidney									
Genes reached maximum intensity at 10 min									
U22520	IP10	2.5	2.2	1.9					
NM_010354	Gelsolin	2.5	1.8	2.0					
NM_012747	STAT3	2.4	1.7	1.4					
L37092	p130 PITSL	2.1	2.1	1.1					
Genes reached maximum intensity at 30 min									
NM_021850	Bak 1	2.4	3.2	1.9					
M61909	NFκB p65	2.1	3.1	2.1					
NM_012752	CD24	1.8	2.8	2.5					
NM_053743	Cdc37	1.8	2.3	1.9					
AF115282	IKKβ	1.9	2.3	1.7					
NM_012967	ICAM-1	1.0	2.2	2.0					
NM_017218	ErbB-3	1.5	2.1	1.7					
NM_017003	HER2	1.3	2.0	1.3					
Genes reached maximum intensity at 60 min									
X06769	c-*fos*	1.5	4.3	4.6					
NM_012551	EGR-I	1.0	2.8	2.9					
Spleen									
Genes reached maximum intensity at 10 min					Genes reached at 0.5-fold at 10 min				
NM_031094	Rb 2 (p130)	3.0	0.7	0.0	AF416291	CD64	0.5	0.6	0.6
AJ441127	FADD	2.1	1.7	0.9	NM_019426	ATFip	0.5	0.6	0.6
X07286	PKC-α	2.1	1.5	2.1	D14014	cyclin D1	0.5	0.4	0.4
NM_031535	Bcl-XL	2.1	1.4	0.7	NM_012747	STAT3	0.4	1.1	0.6
NM_053828	IL-13	2.0	1.8	0.0	AF055291	STAT4	0.4	0.9	0.0
Genes reached maximum intensity at 30 min					NM_080766	N-ras	0.4	0.3	0.3
NM_139194	FAS	1.0	3.1	1.9	NM_133293	GATA-3	0.2	0.1	0.7
L00981	TNF-β	1.6	3.0	1.1	NM_031761	VEGF-D	0.4	0.0	0.0
NM_022177	FGF-2	1.0	3.0	0.0	NM_012789	CD26	0.4	0.0	0.0
NM_011948	MEK Kinase-4	1.2	2.3	1.6	J00750	metallothionein-1	0.3	0.6	0.0
NM_022799	Nucks	2.0	2.1	1.9	U05341	p55 CDC	0.3	0.3	0.0
NM_022799	Nucks	2.0	2.1	1.9	AF072521	PARP	0.3	0.0	0.0
Genes reached maximum intensity at 60 min					AB018576	Cdc7	0.0	0.0	0.0
X06769	c-*fos*	1.2	4.3	6.4	NM_001256	Cdc27	0.0	0.0	0.0
NM_012551	EGR-I	1.6	2.4	5.8	X54419	IL-5	0.0	0.0	0.0
NM_024388	NGF beta	3.4	1.8	3.7	NM_009833	cyclin-T1	0.0	0.0	0.0
L09653	TGFβ-RII	1.1	0.9	2.3	XM_122448	Mat1	0.0	0.0	0.0
D28753	Cdk2-alpha	0.4	0.3	2.2	Genes reached at 0.5-fold at 30 min				
M15562	RT-1Da (MHC Class II)	1.2	1.6	2.0	NM_012923	cyclin G1	0.6	0.5	0.9
					NM_022177	CXCR-4	0.9	0.5	0.7
					NM_013049	OX40	0.9	0.5	0.5
					NM_013091	TNFR1	0.6	0.5	0.3
					NM_012752	CD24	0.7	0.4	0.4
					NM_133572	Cdc25B	0.8	0.4	0.3
					NM_013127	CD38	0.6	0.4	0.3
					NM_011237	Rad9 homolog	0.6	0.3	0.8
					E14273	CD86	1.1	0.0	0.0
					Genes reached at 0.5-fold at 60 min				
					NM_022260	Caspase-7	0.9	0.8	0.4

Mean value of chemiluminescence intensity of GAPDH gene spots diluted at 1/16 on each array filter was used for normalization in the cDNA array experiment. Intensities less than that of a cloning vector fragment as a negative control were cut off from results. Mean values of three independent experiments in duplicate were used as final array results. Genes with changed values over 2-fold or less than 0.5-fold in each tissue with warm ischemia (10, 30, 60 min) against that of each tissue without ischemia (0 min) are shown as affected genes in the table. *GenBank accession no. for mice is shown as that for rats was not available.

terminal deoxynucleotidyl transferase (TdT). The dA-tailed cDNAs were amplified using DNA polymerase KOD Dash® with dNTPs containing biotin-16-dUTP and primer mix including oligo(dT) primer with synthetic anchor sequence. The amplified biotin-labeled cDNAs were used as probes.

Hybridization and detection of signals

The biotin-labeled cDNA probes from each sample were hybridized with the cDNA array filters, using PerfectHyb® Hybridization Solution (TOYOBO Co. Ltd.). Briefly, after prehybridization, the filters were hybridized for overnight with the denatured probes (at 100°C for 5 min) in 10 ml of the hybridization solution at 68°C by rotating at 16 rpm in Hybridization Incubator (Robbins Scientific Co., Sunnyvale, CA, USA). Then the filters were washed three times each with 0.1% sodium dodecyl sulfate (SDS) in 2× SSC solution (1× SCC: 0.15 M sodium citrate, 15 mM citric acid, pH 7.0) at 68°C for 10 min and with 0.1% SDS in 0.1× SSC at 68°C for 5 min. After treating with blocking solution (5% SDS, 125 mM NaCl, 25 mM sodium phosphate, pH 7.2), hybridized signals were developed using Phototope® Star Kit (New England Biolab Inc., Beverly, MA, USA). With Flour S and Quantity One® v4.2.1 software (Bio-Rad Laboratories, Hercules, CA), the chemiluminescence was detected and analyzed using ImaGene™ 4.0 software (BioDiscovery Inc., Segundo, CA, USA). Intensities less than the mean value of signals on spots of the plasmid DNA fragment as a negative control were cut out from results as these were false signals. Mean value of the intensity at spots of glyceraldehyde-3-phosphate dehydrogenase (GAPDH) gene on the filter was used for normalization of each filter. Mean value of each ratio calculated based on the control GAPDH intensity in three rats served as the final result of cDNA array analysis, and the values over 2-fold or less than a half of that in each tissue without ischemia (0 min) were regarded as significant.

Real-time quantitative RT-PCR

The purified total RNAs of each sample described above were reverse-transcribed using a M-MLV RT (Invitrogen). Real-time quantitative PCR was done, using the cDNAs, SYBR Green I dye (SYBR Green PCR Master Mix; Applied Biosystems), and primer sets, 5'-CACTCC-CAGCTGCACTACCTAT-3' and 5'-GCGAGCTCAGT-GAGTCAGAG-3' for rat c-fos (GenBank accession no. X06769), 5'-TACCTACCCGTCTCCTGCAC-3' and 5'-GAGGTGCTGAAGGAGTTGCT-3' for rat early growth response-1 (Egr-1) (GenBank accession no. NM-012551), and 5'-CCGGCTAGAGGAAAAAGTGA-3' and 5'-TGAGTTGGCACCCACTGTTA-3' for rat c-jun (GenBank accession no. X17163). As internal controls, the expression levels of rat GAPDH and β-actin genes in each sample were

examined using primer sets, 5'-ATGGGAGTTGCTGTT-GAAGTCA-3' and 5'-CCGAGGGCCCACTAAAGG-3' for GAPDH (GenBank accession no. NM-017008), and 5'-TGTGTGGATTGGTGGCTCTATC-3' and 5'-CATCG-TACTCCTGCTTGCTGATC-3' for β-actin (GenBank accession no. NM-031144). PCR was done at 45 cycles of two-step reaction (95°C for 30 s, 60°C for 30 s) after the initial denaturation (95°C, 15 min), using an ABI PRISM 7000 Sequence Detector System (Applied Biosystems). The amount of specific mRNA was quantified at the point where the system detected the uptake in exponential phase of PCR accumulation and ratio to that of GAPDH gene was calculated for each sample.

Immunohistochemical analysis

Four-micron sections of formalin-fixed paraffin-embedded tissues from three rats in each experiment were immunostained with monoclonal antibodies against rat c-fos (sc-52, Santa Cruz Biotechnology, Inc. Santa Cruz, CA, USA), Ki-67 (MIB-5, Dako Cytomation, Glostrup, Denmark) and single-strand DNA (ssDNA, Dako Cytomation), using a LSAB2 Kit/HRP (Dako Cytomation).

Results

Modulation of gene expression in tissues with warm ischemia

To evaluate chronological and tissue-specific modulation of gene expression by warm ischemia after surgical extirpation, we analyzed expression of several genes related to apoptosis, regulation of cell cycle, and signal transduction in four major tissues, lung, liver, kidney, and spleen of rats, which were left at room temperature for 10, 30, or 60 min, using an original cDNA array system. Quality of total RNAs in each sample was confirmed to be a high level regardless of warm ischemia within 60 min (Fig. 1). However, the cDNA array showed that expression of many genes was modulated by warm ischemia within 60 min in all tissues tested, 19.1% of 271 genes in lung, 11.0% in liver, 5.1% in kidney and 16.2% in spleen, and that many of these genes were affected within 10 min after surgical extirpation regardless of the kind of tissues, 44.2% of the affected genes in lung, 50.0% in liver, 28.5% in kidney, and 50.0% in spleen (Table 1). A few genes in each tissue, such as c-fos, Egr-1 and matrix metalloproteinase (MMP-2) in lung, and c-fos and Egr-1 in spleen, showed extremely high expression (over 5-fold increase). The number of down-regulated genes in each tissue with warm ischemia varied. A large number of down-regulated genes (less than a half of each expression at "0 min" control) were observed in lung (51.9% of the affected genes) and spleen (63.6%), but only few or no genes were down-regulated by warm ischemia in liver

(6.6%) or kidney (0%), respectively (Table 1). No gene had common expression pattern among four tissues with warm ischemia in our cDNA array. Interestingly, some genes showed contrary response among them; for example, the expressions of metallothionein-1 and cyclin D1 genes increased in lung but were reduced in spleen. Both expressions of c-*fos* and Egr-1, which are family of immediately early genes (IEGs) and are known to be induced under conditions of ischemic stress similar as other genes of the family (Aebert et al., 1997), gradually increased and reached remarkably high levels (more than 5-fold) at 60 min after surgical extirpation of lung and spleen, but no similar pattern was seen in liver although increment of Egr-1 expression (2.5-fold) at 10 min was observed. In kidney with warm ischemia, elevation of both c-*fos* and Egr-1 expressions was found, but the levels were less than a half of those in lung and spleen (data not shown).

Quantitative analysis of mRNA expression of c-fos, Egr-1 and c-jun in tissues with warm ischemia determined using real time RT-PCR

To confirm the tissue specific induction of the expression of IEGs including c-*fos* and Egr-1 by warm ischemia, the expression levels in each tissue left at room temperature for 60 min were compared to those of "0 min" control by real time quantitative RT-PCR (Fig. 2). Furthermore, c-*jun*, another component of the AP-1 transcriptional factor complex than c-*fos*, was also examined, although our array filter did not carry this gene. The expression of c-*fos*, Egr-1 and c-*jun* was significantly increased in lung (15.4-fold, 9.1-fold, and 4.7-fold, respectively) with warm ischemia, but not in liver (1.5-fold, 0.9-fold, and 0.8-fold) (Fig. 2). In

kidney and spleen, the levels of c-*fos*, Egr-1, and c-*jun* were low, although the expression was increased 4.4-fold, 4.0-fold and 1.5-fold, and 11.1-fold, 4.2-fold and 3.5-fold, respectively.

Increment of c-fos protein production in epithelial cells of bronchioles in lung with warm ischemia

To determine the localization of c-*fos* protein in situ, immunohistochemical staining was done on each tissue section with or without warm ischemia. In lung, c-*fos* protein was faintly expressed in the bronchiole epithelial cells under nonischemic condition, and the expression increased gradually after the start of warm ischemia. An abundant expression of c-*fos* protein was observed in the epithelium at 60 min after the extirpation (Fig. 3). On the other hand, c-*fos* protein in liver was distinct only in bile duct epithelial cells of portal tracts at similar staining levels regardless of warm ischemia, although a nonspecific pale staining was seen in hepatocytes (Fig. 3). In kidney, c-*fos* protein was detected in the epithelium of proximal tubules. Staining in spleen was not specified regardless of conditions with or without warm ischemia because abundant non-specific staining was found in red blood cells (data not shown).

Increment of apoptotic cells in lung with warm ischemia

To determine if the increment of IEGs expression in lung with warm ischemia would affect kinetics of bronchiolar epithelial cells, immunohistochemistry, using the monoclonal anti-Ki-67 (MIB-1 for cell proliferation marker) and anti-ssDNA (for detection of apoptotic cells) antibodies, was done. Numbers of Ki-67-positive cells started to decrease at
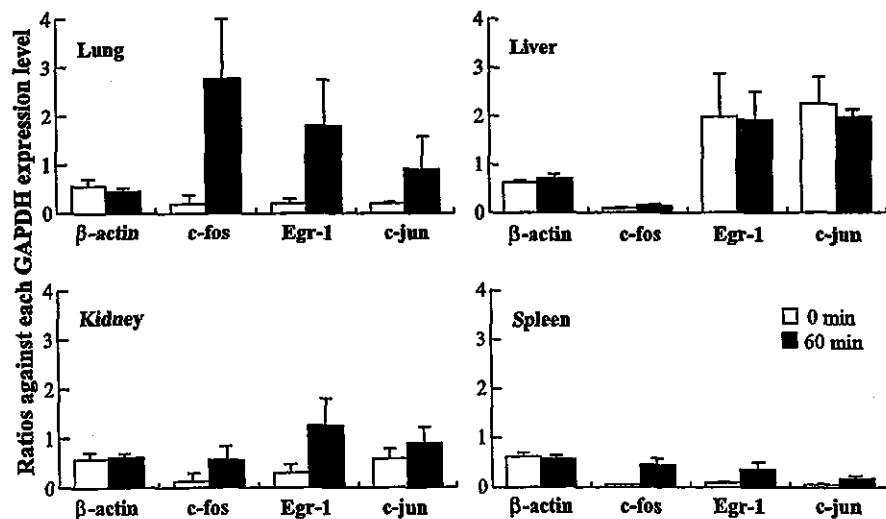
Fig. 2. Differential modulation of immediate early genes among organs with warm ischemia. To confirm the differential expression of c-*fos*, Egr-1 or c-*jun* mRNA, real-time quantitative RT-PCR was done and the levels of mRNA expression in samples with 60 min warm ischemia were compared with that of each control without ischemia (0 min). The β-actin gene was served as a house-keeping control. Data represented relative intensity to expression levels of GAPDH mRNA in each sample. Values are mean ratio ± SD in three independent experiments, which were done in triplicates.
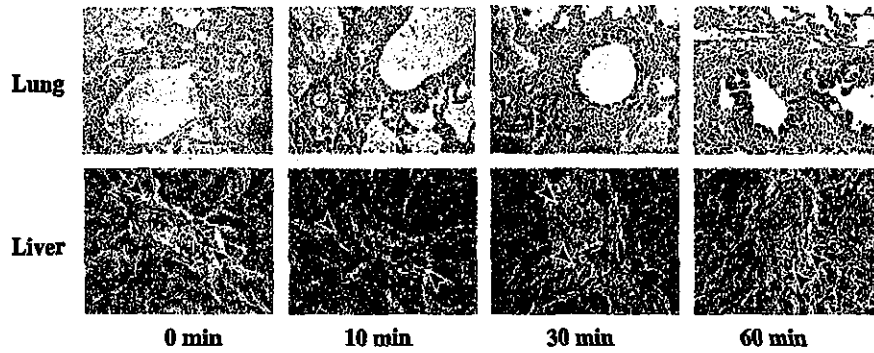
Fig. 3. (A) Immunohistochemical staining of c-fos protein in tissues with warm ischemia. Using an anti-c-fos antibody, tissues with or without warm ischemia were immunostained. Representative results of lung, which showed significant increment of c-fos mRNA expression by ischemic stress, and of liver, which showed no specific increment, are shown. Zero minute means tissues without ischemia, and 10, 30, and 60 min mean time exposed to warm ischemia. Arrows in liver indicate bile ducts consistently expressed c-fos in their epithelial cells.
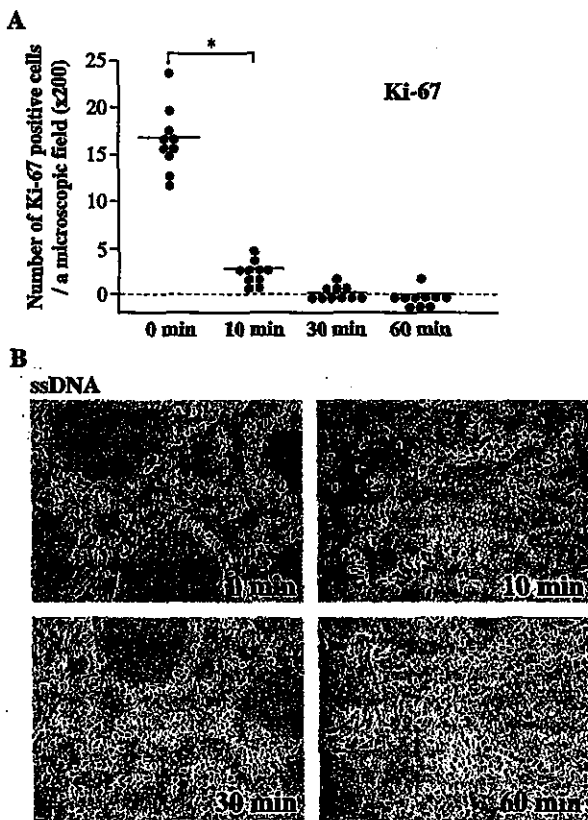
Fig. 4. Kinetics of bronchiolar epithelium in lung with warm ischemia. (A) Proliferation activity in lung tissue was measured by number of Ki-67-positive cells in immunohistochemical staining. After an immunostaining for rat Ki-67, number of positive cells was counted in a field of microscope at ×200 in magnification. Samples divided from three rats were tested under each condition and three fields were counted in each sample. Each circle shows positive cell number in each field and bar means the average number in each condition. *$P < 0.01$ compared to 0 min (Student's t test). (B) Apoptotic cells in lung were detected in immunohistochemistry using an anti-ssDNA antibody. Representative results are shown. Zero minute means tissues without ischemia, and 10, 30, and 60 min mean time exposed to warm ischemia.

10 min after the extirpation and almost disappeared at 30 min (Fig. 4A). An abundant number of ssDNA-positive cells was evident in the bronchiolar epithelium with warm ischemia similar to the result of c-fos immunostaining (Fig. 4B), suggesting that these cells were undergoing to apoptotic cell death and that the apoptosis might be related with c-fos expression. In other tissues, no Ki-67-positive cell was evident. ssDNA-positive cells in kidney tended to increase after starting warm ischemia, and no significant change in the cell number was found in liver and spleen (data not shown).

Discussion

cDNA arrays enable monitoring the mRNA expression of thousands of genes, simultaneously. Consequently, the technology revealed a large degree of variability in gene expression patterns on particular tissues, but the variability has often been attributed to genetically different individuals. Huang et al. (2001) noticed the effects of ischemia on gene expression profile probed by cDNA microarrays using tissue samples of human normal mucosa. Differential gene expression related to duration of warm ischemia was noted in samples of radical prostatectomy, using a cDNA microarray (Dash et al., 2002). These reports suggested that some of results previously reported using cDNA array technology might have included effects by secondary changes such as ischemia.

Although no remarkable change of the mRNA quality was evident in all rat tissues we tested, expression of many genes was modulated within 60 min after starting warm ischemia. In lung and spleen, many genes were listed as up- or down-regulated genes. However, only two or no genes were listed as down-regulated genes in liver or kidney, respectively, although several genes were up-regulated in both tissues. These observations suggest that warm ischemia might differentially impact organs, and that lung and

spleen might be more sensitive to mRNA degradation induced by warm ischemia. Expression of c-fos, c-jun, and Egr-1 genes known as IEGs was induced rapidly and transiently in most tissues after a wide variety of chemical and physical extracellular stresses (Aebert et al., 1997; Deindl et al., 2003; Gess et al., 1997; Ogawa et al., 1996; Safirstein et al., 1990). Induction of IEGs by ischemia–reperfusion injury was demonstrated in various tissues using animal models (Amberger et al., 2002; Bonventre et al., 1991; Schlossberg et al., 1996; Yoshimura et al, 2003). Expression of c-fos and c-jun in kidney with ischemia by the hilar clumping increased rapidly within 50 min as a stress response (Megyesi et al., 1995). In the present study on rat tissues, the elevation of both c-fos and Egr-1 expressions in kidney was found in cDNA array and real-time quantitative RT-PCR. In addition, c-fos staining in kidney tissue tended to increase after start of ischemia. However, in liver, 20 h but not 0.5h cold ischemia and reperfusion was needed to induce increment of c-fos and c-jun expression (Wieland et al., 2000), thus, corresponding to our result that expression of IEGs, including c-fos, in liver was not induced by ischemic stress within 60 min. These findings suggest that liver may have highly resistant activity against ischemic stress in comparison with other organs. IEGs play important roles in cell proliferation. The AP-1 transcription factor composed of c-fos and c-jun induces genes which not only stimulate S phase entry and cell cycle progression but also involved in the activation of programmed cell death (Shaulian and Karin, 2001). In lung with warm ischemia, abundant positive staining for ssDNA was evident in bronchiolar epithelium where c-fos was detected, suggesting that AP-1 might induce apoptotic cell death in the bronchiolar epithelium. Actually, TNF-α and cyclin D1, which are targets for AP-1 and induce apoptotic cell death (Freeman et al., 1994; Guo et al., 2002), were up-regulated in lung with warm ischemia (see Table 1). Egr-1 functions as a master switch activated by ischemia, and many of chemokines, adhesion receptors, procoagulants and permeability-related genes are coordinately up-regulated by Egr-1 under conditions with rapid ischemia (Yan et al., 2000). In line with this observation, the finding that many genes were up-regulated in rat tissues with warm ischemia in our cDNA array analysis should not be surprising.

On the other hand, mRNA stability and half-life also work as an influential factor of quantitative levels of mRNA expression, and stresses may induce prolonged or a shorter half-life of mRNA depending on the species of genes, cell types, and/or kind of stress. Although several pathways to mRNA decay have been demonstrated, little is known of the specific stability and half-life of each mRNA (Guhaniyogi and Brewer, 2001; Wagner and Andersen, 2002). Therefore, gene-specific mRNA stability and half-life cannot be considered here, although the quality of total RNAs until 60 min after the extirpation was confirmed to be in similar levels as "0 min" control. Characteristics of each mRNA can

also be considered in future studies of gene expression carried out under varied conditions.

In conclusion, our results demonstrate that genes may show tissue-dependent differential transcriptional response against warm ischemia. Tissue samples obtained from patients during surgery cannot completely escape effects of ischemia. Therefore, researchers using clinical samples should recognize the genes that are easily affected by artificial stress, such as warm ischemia. In case of examination by cDNA array analysis, biologists should keep in mind that tissue samples come equipped with particular footprints.

Acknowledgments

References

Aebert, H., Cornelius, T., Her, T., Holmer, S.R., Birnbaum, D.E., Riegger, G.A., Schunkert, H., 1997. Expression of immediate early genes after cardioplegic arrest and reperfusion. Ann. Thorac. Surg. 63, 1669–1675.

Amberger, A., Schneeberger, S., Hernegger, G., Brandacher, G., Obrist, P., Lackner, P., Margreiter, R., Mark, W., 2002. Gene expression profiling of prolonged cold ischemia and reperfusion in murine heart transplants. Transplantation 74, 1441–1449.

Bertucci, F., Viens, P., Tagett, R., Nguyen, C., Houlgatte, R., Birnbaum, D., 2003. DNA arrays in clinical oncology: promises and challenges. Lab. Invest. 83, 305–316.

Bonventre, J.V., Sukhatme, V.P., Bamberger, M., Ouellette, A.J., Brown, D., 1991. Localization of the protein product of the immediate early growth response gene, Egr-1, in the kidney after ischemia and reperfusion. Cell Regul. 2, 251–260.

Brand, T., Sharma, H.S., Fleischmann, K.E., Duncker, D.J., McFalls, E.O., Verdouw, P.D., Schaper, W., 1992. Proto-oncogene expression in porcine myocardium subjected to ischemia and reperfusion. Circ. Res. 71, 1351–1360.

Bunney, W.E., Bunney, B.G., Vawter, M.P., Tomita, H., Li, J., Evans, S.J., Choudary, P.V., Myers, R.M., Jones, E.G., Watson, S.J., Akil, H., 2003. Microarray technology: a review of new strategies to discover candidate vulnerability genes in psychiatric disorders. Am. J. Psychiatry 160, 657–666.

Dash, A., Maine, I.P., Varambally, S., Shen, R., Chinnaiyan, A.M., Rubin, M.A., 2002. Changes in differential gene expression because of warm ischemia time of radical prostatectomy specimens. Am. J. Pathol. 161, 1743–1748.

Deindl, E., Kolar, F., Nebulae, E., Vogel, S., Schaper, W., Ostadal, B., 2003. Effect of intermittent high altitude hypoxia on gene expression in rat heart and lung. Physiol. Res. 52, 147–157.

Freeman, R.S., Estus, S., Johnson Jr., E.M., 1994. Analysis of cell cycle-related gene expression in postmitotic neurons: selective induction of Cyclin D1 during programmed cell death. Neuron 12, 343–355.

Gerhold, D.L., Jensen, R.V., Gullans, S.R., 2002. Better therapeutics through microarrays. Nat. Genet. 32, 547–551.

Gess, B., Wolf, K., Pfeifer, M., Riegger, G.A., Kurtz, A., 1997. In vivo carbon monoxide exposure and hypoxic hypoxia stimulate immediate early gene expression. Pflüegers Arch.-Eur. J. Pysiol. 434, 568–574.

Goto, S., Matsumoto, I., Kamada, N., Bui, A., Saito, T., Findlay, M., Pujic, Z., Wilce, P., 1994. The induction of immediate early genes on postischemic and transplanted livers in rats: Its relation to organ survival. Transplantation 58, 840–845.

Guhaniyogi, J., Brewer, G., 2001. Regulation of mRNA stability in mammalian cells. Gene 265, 11–23.

Guo, R.F., Lentsch, A.B., Sarma, J.V., Sun, L., Riedemann, N.C., McClintock, S.D., McGuire, S.R., Van-Rooijen, N., Ward, P.A., 2002. Activator protein-1 activation in acute lung injury. Am. J. Pathol. 161, 275–282.

Huang, J., Qi, R., Quackenbush, J., Dauway, E., Lazaridis, E., Yeatman, T., 2001. Effects of ischemia on gene expression. J. Surg. Res. 99, 222–227.

Itoh, H., Yagi, M., Fushida, S., Tani, T., Hashimoto, T., Shimizu, K., Miwa, K., 2000. Activation of immediate early gene, c-fos, and c-jun in the rat small intestine after ischemia/reperfusion. Transplantation 69, 598–604.

Megyesi, J., Di-Mari, J., Udvarhelyi, N., Price, P.M., Safirstein, R., 1995. DNA synthesis is dissociated from the immediate-early gene response in the post-ischemic kidney. Kidney Int. 48, 1451–1458.

Ogawa, Y., Saibara, T., Terashima, M., Ono, M., Hamada, N., Nishioka, A., Inomata, T., Onishi, S., Yoshida, S., Seguchi, H., 1996. Sequential alteration of proto-oncogene expression in liver, spleen, kidney and brain of mice subjected to whole body irradiation. Oncology 53, 412–416.

Plumier, J.C., Robertson, H.A., Currie, R.W., 1996. Differential accumulation of mRNA for immediate early genes and heat shock genes in heart after ischemic injury. J. Mol. Cell. Cardiol. 28, 1251–1260.

Safirstein, R., Price, P.M., Saggi, S.J., Harris, R.C., 1990. Changes in gene expression after temporary renal ischemia. Kidney Int. 37, 1515–1521.

Sakai, T., Takaya, S., Fukuda, A., Harada, O., Kobayashi, M., 2003. Evaluation of warm ischemia-reperfusion injury using heat shock protein in the rat liver. Transpl. Int. 16, 88–99.

Schlossberg, H., Zhang, Y., Dudus, L., Engelhardt, J.F., 1996. Expression of c-fos and c-jun during hepatocellular remodeling following ischemia/reperfusion in mouse liver. Hepatology 23, 1546–1555.

Shaulian, E., Karin, M., 2001. AP-1 in cell proliferation and survival. Oncogene 20, 2390–2400.

Wagner, E., Andersen, J.L., 2002. mRNA surveillance: the perfect persist. J. Cell Sci. 115, 3033–3038.

Wieland, E., Oellerich, M., Braun, F., Schütz, E., 2000. c-fos and c-jun mRNA expression in a pig liver model of ischemia/reperfusion: effect of extended cold storage and the antioxidant idebenone. Clin. Biochem. 33, 285–290.

Yan, S.F., Fujita, T., Lu, J., Okada, K., Shan-Zou, Y., Mackman, N., Pinsky, D.J., Stern, D.M., 2000. Egr-1, a master switch coordinating upregulation of divergent gene families underlying ischemic stress. Nat. Med. 12, 1355–1361.

Yoshimura, N., Kikuchi, T., Kuroiwa, S., Gaun, S., 2003. Differential temporal and spatial expression of immediate early genes in retinal neurons after ischemia-reperfusion injury. Invest. Ophthalmol. Visual Sci. 44, 2211–2220.

ORIGINAL ARTICLE

Bone marrow cells carrying the env-pX transgene play a role in the severity but not prolongation of arthritis in human T-cell leukaemia virus type-I transgenic rats: a possible role of articular tissues carrying the transgene in the prolongation of arthritis

Asami Abe[*†], Akihiro Ishizu[*], Hitoshi Ikeda[*], Hiroko Hayase[*], Takahiro Tsuji[*], Yukiko Miyatake[*], Muneharu Tsuji[*†], Kazunori Fugo[*], Toshiaki Sugaya[*], Masato Higuchi[*], Takeo Matsuno[†] and Takashi Yoshiki[*]

Department of Pathology/Pathophysiology, Division of Pathophysiological Science, Hokkaido University Graduate School of Medicine, Sapporo, Japan, and †Department of Orthopedics, Asahikawa Medical College, Asahikawa, Japan

INTERNATIONAL
JOURNAL OF
EXPERIMENTAL
PATHOLOGY

Summary

Transgenic rats carrying the *env-pX* gene of human T-cell leukaemia virus type-I (env-pX rats) were immunized with type II collagen (CII), and chronological alterations of arthritis were compared with findings of collagen-induced arthritis (CIA) in wildtype Wistar–King–Aptekman–Hokudai (WKAH) rats. Arthritis induced by CII in env-pX rats was more severe and persisted longer than CIA in WKAH rats. To determine whether the phenomenon is caused mainly by the transgene-carrying lymphocytes or articular tissues, we immunized lethally irradiated env-pX and WKAH rats with reciprocal bone marrow cell (BMC) transplantation. A severe but transient arthritis was induced by CII in WKAH rats reconstituted by env-pX BMC (w/tB/CII rats). On the other hand, in env-pX rats reconstituted by WKAH BMC, arthritis persisted longer than in w/tB/CII rats, although the degree was less at an early phase after CII immunization. These findings suggest that articular tissues rather than the BMCs carrying the *env-pX* transgene play a role in the prolongation of arthritis in env-pX rats, although BMCs carrying the transgene are associated with the severity of arthritis. When inflammatory cytokines in synovial cells isolated from env-pX rats before they developed arthritis were examined, interleukin-6 (IL-6) was detected at a higher level than in synovial cells from WKAH rats, thus suggesting the critical role of IL-6 in env-pX arthritis.

Keywords

animal model, arthritis, HTLV-I, IL-6, synovial cells

Human T-cell leukaemia virus type-I (HTLV-I) is the pathogenetic agent of adult T-cell leukaemia (Poiesz *et al.* 1980; Yoshida *et al.* 1982) and is also associated with many inflammatory diseases, including myelopathy (Gessain *et al.* 1985; Osame *et al.* 1986), uveitis (Mochizuki *et al.* 1992) and, probably, arthropathy (Nishioka *et al.* 1989), Sjögren's syndrome

(Vernant et al. 1988), T-cell alveolitis (Sugimoto et al. 1987; Vernant et al. 1988) and infective dermatitis (LaGrenade et al. 1990). Because Tax encoded by HTLV-I pX gene modulates the expression and function of host molecules such as cytokines, cytokine receptors, growth factors, transcription factors and cell-cycle-related molecules, the pX gene may play the major pathogenetic roles in HTLV-I-associated diseases (Arima & Tei 2001; Johnson et al. 2001). To investigate the pathogenetic roles of HTLV-I in vivo, we established several HTLV-I transgenic rat models (Yamada et al. 1995; Yamazaki et al. 1997; Kikuchi et al. 2002). Among them, Wistar–King–Aptekman–Hokudai (WKAH) rats expressing the env-pX transgene constitutively in systemic organs under control of the viral long-terminal repeat promoter (env-pX rats) developed chronic destructive arthritis and other collagen vascular diseases (Yamazaki et al. 1997, 1998; Nakamaru et al. 2001; Fugo et al. 2002; Sugaya et al. 2002; Higuchi et al. 2003). Because rheumatoid factors and anti-nuclear and anti-DNA autoantibodies were present in sera, env-pX rats seem to be a suitable model for human autoimmune diseases, including rheumatoid arthritis. Before development of diseases, peripheral T-cells were pre-activated to express intercellular adhesion molecule-1 and CD80/86 and showed a hyper-response against several mitogenic stimuli in vitro (Nakamaru et al. 2001). When arthritides of env-pX rats were compared with those of collagen-induced arthritis (CIA) in nontransgenic WKAH rats, we found that cellular and humoral immune responses differed between the two (Sugaya et al. 2002).

For further characterization of arthritides, we immunized env-pX and WKAH rats with type II collagen (CII) and a chronological study of CIA concerning histological severity and disease persistence was undertaken. Arthritis induced by CII in env-pX rats was more severe and persisted longer than CIA in WKAH rats. To clarify whether the phenomenon is caused mainly by the transgene-carrying lymphocytes or articular tissues, we induced arthritis by CII immunization in lethally irradiated env-pX and WKAH rats with reciprocal bone marrow cell (BMC) transplantation. In addition, synovial cells were isolated from env-pX rats before they developed arthritis, and the production of inflammatory cytokines in the cells was compared with that in synovial cells from WKAH rats.

Materials and methods

Rats

Male WKAH rats and env-pX rats (WKAH rats bearing the env-pX gene; Yamazaki et al. 1997) that did not have macroscopically recognizable diseases were used. These rats were maintained at the Institute for Animal Experimentation, Hokkaido University Graduate School of Medicine. Experiments using animals were performed in accordance with the guidelines for the care and use of laboratory animals in Hokkaido University Graduate School of Medicine.

BMC transfer

Mononuclear cells were separated from the bone marrow of env-pX and WKAH rats (6 weeks old), using Lympholyte Rat (Cedarlane, Hornby, Ontario, Canada). All env-pX rats that served as BMC donors were confirmed microscopically to be disease free. BMCs (1×10^7/rat) were injected via the tail vein of recipient rats (6 weeks old) which had been lethally irradiated at 12 Gy by ^{60}Co.

Immunization with CII

Bovine CII (Nitta Gelatin, Osaka, Japan) was dissolved in phosphate-buffered saline at a concentration of 3 mg/ml, and an equal volume of complete Freund's adjuvant (Difco, Detroit, MI, USA) was added to the mixture. The emulsion was singly injected into the subcutis of the tail root (667 µl/rat).

Histological scoring of arthritis

Histological score of arthritis was determined according to methods described by Koizumi (1999) but with modifications. Four criteria, including infiltration of inflammatory cells (scores 0–4), proliferation of stroma (scores 0–4), fibrosis (scores 0–3) and proliferation of synovial lining cells (scores 0–3), were evaluated (Figure 1 and Table 1).

Lymphocyte proliferation assay in vitro

Lymph node cells (4×10^5/well) from CII-immunized env-pX and WKAH rats were incubated in 96-well round-bottom plates for 96 h with 0, 0.1, 5, 10, 25 or 100 µg/ml of CII which had been heat degenerated at 56 °C for 30 min. [^{3}H]-Thymidine (18.5 kBq) was pulsed for 16 h before harvest of the cells. Proliferation of lymphocytes was quantified by [^{3}H]-thymidine uptake.

Microdissection and nested polymerase chain reaction

To detect the env-pX transgene in lymphocytes accumulating at arthritic joints, 1000 lymphocytes were dissected from formalin-fixed, paraffin-embedded sections by laser-captured microdissection LM200 (Arcturus, Mountain View, CA, USA), and nested polymerase chain reaction (PCR) was carried out according to methods described by Fugo et al. (2002).

Table 1 Histological scoring of arthritis

	Score				
	0	1	2	3	4
Infiltration of inflammatory cells	None	Mild	Moderate	Severe, diffuse	Severe, granulomatous
Proliferation of stroma	None	Neovascularization	Granulation	Pannus	Pannus and periarticular oedema
Fibrosis	None	Mild	Moderate	Severe	NA
Proliferation of lining cells (layers)	1-2	3-4	5-6	>7	NA

NA, score not applied.

Cultivation of synovial cells

Synovial cells were isolated from 6-week-old WKAH rats and env-pX rats before they developed arthritis, according to methods described by Ishizu *et al.* (2003). Because the cultured cells were immunocytochemically negative for markers of type A (macrophage-like) cells such as lysozyme, α1-antitrypsin or α1-antichymotrypsin, we considered that the cells have type B (fibroblastic) characteristics.

Enzyme-linked immunosorbent assay

Interleukin-1α (IL-1α), IL-1β, IL-2, IL-6, tumour necrosis factor-α (TNF-α) and interferon-γ (IFN-γ) in culture supernatants of rat synovial cells were measured using enzyme-linked immunosorbent assay (ELISA) kits (Amersham Pharmacia Biotech, Piscataway, NJ, USA).

Real-time reverse transcriptase polymerase chain reaction

For a quantitative analysis of mRNA expression of IL-6, real-time reverse transcriptase polymerase chain reaction (RT-PCR) was performed using QuantiTect SYBR Green

PCR (Qiagen, Hilden, Germany), according to methods described by Ishizu *et al.* (2003). Primers for IL-6 used were 5′-attgaaaatctgctctggtcttctg-3′ (sense) and 5′-ctggct ttgtctttcttgttatcttg-3′ (antisense). The size of the amplicon was 90 bp. Data were analysed using ABI PRISM 7900HT (Applied Biosystems, Foster City, CA, USA).

Statistics

Results are shown as mean ± standard deviation. Mann–Whitney U-test was used for statistical analysis. P-Value under 0.05 was considered to be significant.

Results

Comparison of arthritis induced by CII immunization in env-pX and WKAH rats

WKAH and env-pX rats were immunized with CII. In both groups, ankle joints of all rats swelled at around 10 days after CII immunization (Figure 2). Approximately 80% of env-pX rats naturally develop arthritis usually after 3 months of age,
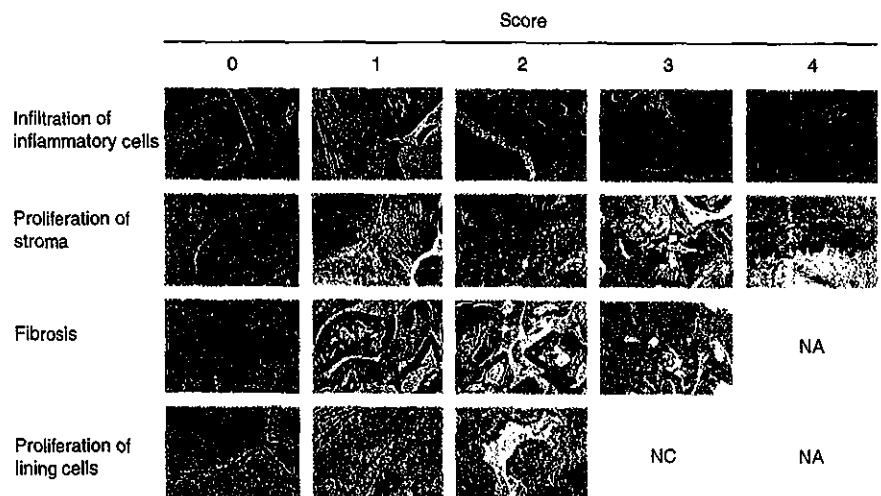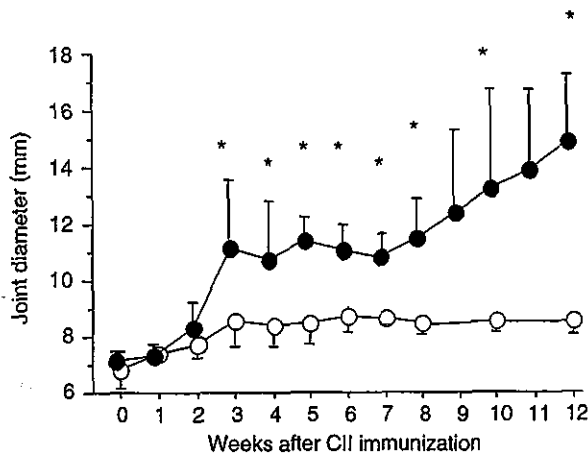

Figure 1 Representative photographs that correspond with the scores summarized in Table 1 are shown. NA, score not applied; NC, no corresponding case.

Figure 2 Chronological change of diameter of ankle joints. In each group, eight rats were immunized with type II collagen (CII), and then at 2, 4, 8 and 12 weeks after immunization, two rats were killed at random. Data from both right and left ankles of alive rats are shown. ●, env-pX rats; ○, WKAH rats. *P < 0.01.

and the age of onset differs from rat to rat. Because all env-pX rats immunized with CII equally manifested joint swelling within 2 weeks (2 months old), it might be reasonable to consider that they developed CIA. At 3 weeks after immunization, ankle joints of env-pX rats (diameter = 11.63 ± 5.67 mm) were significantly larger than those of WKAH rats (diameter = 8.59 ± 0.83 mm, P = 0.004). The diameter of env-pX joints further increased after 8 weeks after immunization, whereas that of WKAH joints did not (diameter at 12 weeks after immunization: env-pX, 15.35 ± 5.18 mm; WKAH, 8.57 ± 0.27 mm; P = 0.004). A marked infiltration of inflammatory cells was evident in arthritic joints of both env-pX and WKAH rats at 2 weeks after immunization (Figure 3a). An equivalent degree of inflammatory cell infiltration persisted in env-pX rats; however, the numbers of inflammatory cells accumulating at arthritic joints decreased in WKAH rats (at 12 weeks after immunization: env-pX score, 3.0 ± 2.0; WKAH score, 0.3 ± 0.2; P = 0.0089). A similar phenomenon was observed regarding the proliferation of stroma (at 12 weeks after immunization: env-pX score, 4.0 ± 0.0; WKAH score: 2.2 ± 0.4; P = 0.0046) (Figure 3b). There was a time-dependent augmentation of fibrosis (Figure 3c). The score for env-pX rats (3.0 ± 0.0) was higher than that for WKAH rats (1.9 ± 0.5) at 12 weeks after immunization (P = 0.0237). There was no significant difference in the proliferation of synovial lining cells between env-pX and WKAH rats, and most synovial lining cells disappeared when fibrosis progressed (Figure 3d). Representative photographs of arthritic joints at 4 and 12 weeks after CII immunization are shown in Figure 4.
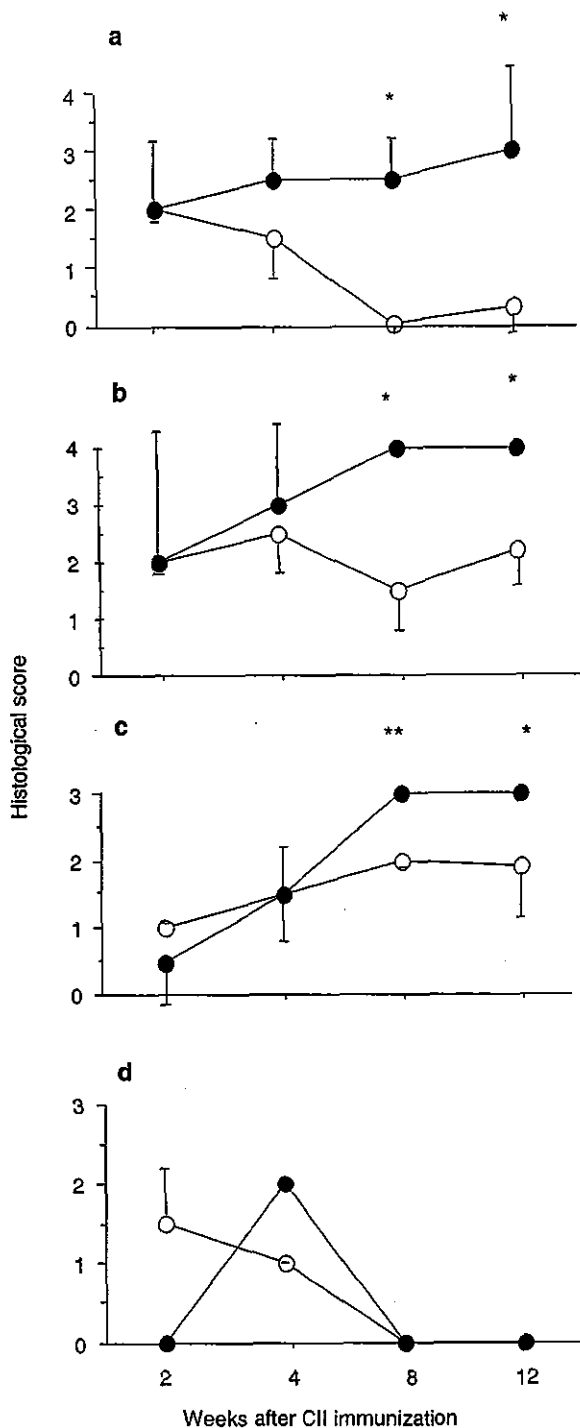
Figure 3 Histological score of arthritis. Infiltration of inflammatory cells (a), proliferation of stroma (b), fibrosis (c) and proliferation of synovial lining cells (d) were evaluated as indicated in Figure 1. At each time point, data from four ankles of two rats are shown. ●, env-pX rats; ○, WKAH rats. *P < 0.01, **P < 0.05.
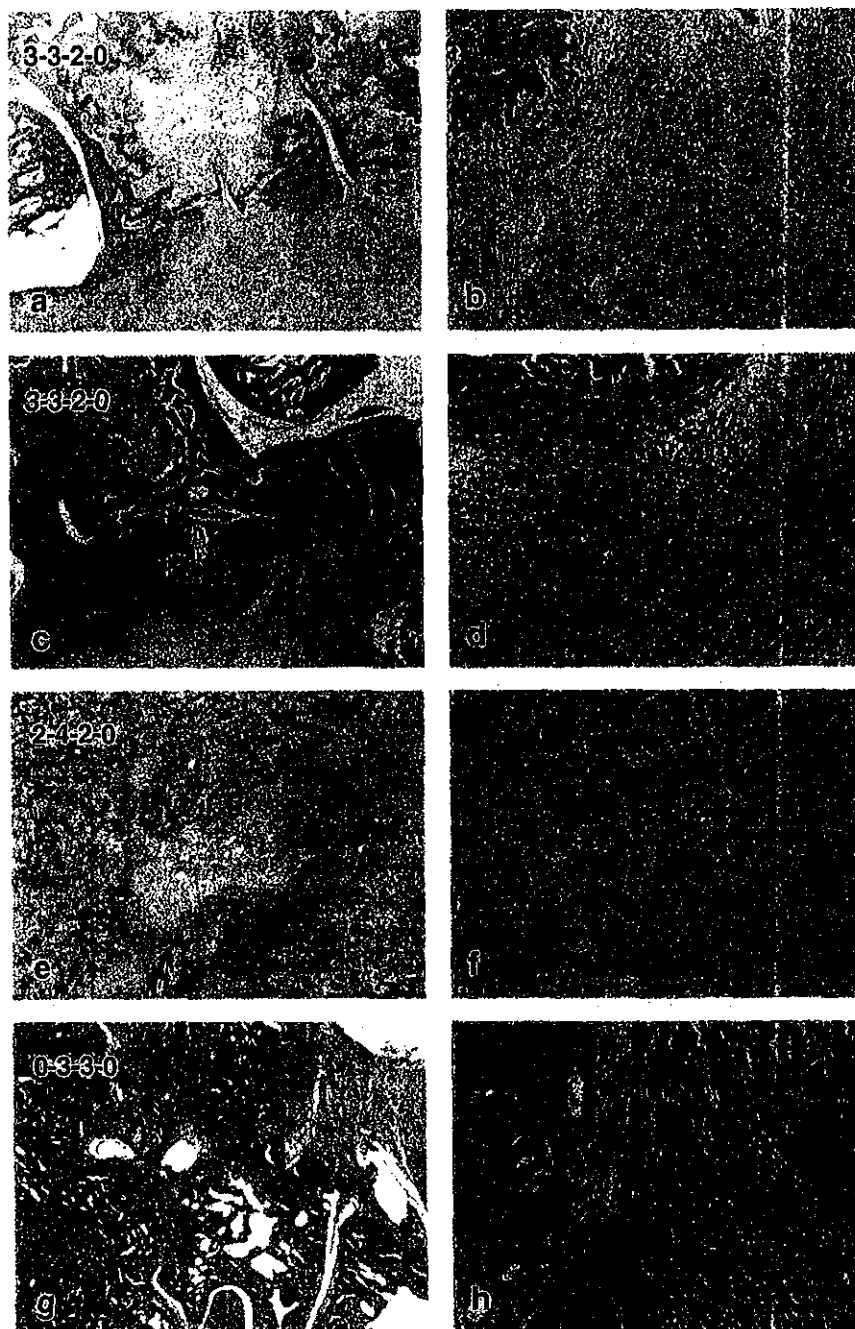
Figure 4 Representative photographs of arthritic joints of env-pX (a, b, e, f) and WKAH (c, d, g, h) rats at 4 (a–d) and 12 (e–h) weeks after type II collagen (CII) immunization. The right panels represent views of high-power field (original magnification, ×100) of the left panels (×20). The four numbers in the left panels, from left to right, represent histological scores for infiltration of inflammatory cells, proliferation of stroma, fibrosis and proliferation of synovial lining cells, respectively.

Comparison of in vitro lymphocyte proliferation against CII in env-pX and WKAH rats that had been immunized with CII

Because Wistar-King-Aptekman (WKA) strains, including WKAH rats, were low responders for adjuvant arthritis (Kayashima et al. 1976), we considered that T-cell responses against CII might be evident in WKAH rats with CIA. *In vitro* proliferation of lymphocytes against CII was assayed in CII-immunized WKAH rats, and the findings were compared with those of CII-immunized env-pX rats. Lymphocytes from CII-immunized env-pX rats showed significantly higher and dose-dependent responses by addition of CII than those of cells from CII-immunized WKAH rats (Figure 5).
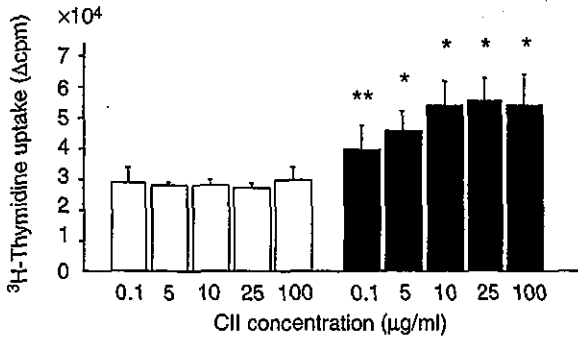
Figure 5 In vitro responsiveness to type II collagen (CII) of lymphocytes from CII-immunized env-pX rats (■) and WKAH controls (□). Heat-degenerated CII was added into the cell culture, as indicated. Data are shown as augmentation of [³H]-thymidine uptake (Δcpm). Δcpm = [³H]-thymidine uptake when CII added - [³H]-thymidine uptake without CII. Experiments were carried out in triplicate more than three times. The representative results are shown. *P < 0.01, **P < 0.05.

Comparison of arthritis induced by CII immunization in env-pX and WKAH rats with reciprocal BMC transfer

By 8 weeks after CII immunization, ankle joints of WKAH rats reconstituted by env-pX BMC (w/tB/CII rats) showed severe swelling (Figure 6), as seen in env-pX rats (Figure 2). On the other hand, the early-phase response in env-pX rats reconstituted by WKAH BMC (t/wB/CII rats) was similar to that in WKAH rats. There was a significant difference between w/tB/CII and t/wB/CII rats (diameter of joints at 4
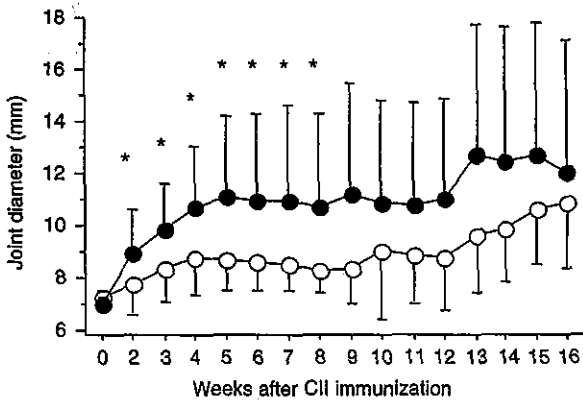

Figure 6 Chronological change of diameter of ankle joints. In each group, 20 rats were immunized with type II collagen (CII), and then at 4, 8, 12 and 16 weeks after immunization, five rats were killed at random. Data from both right and left ankles of alive rats are shown. ●, WKAH rats reconstituted by env-pX BMC (w/tB/CII rats); O, env-pX rats reconstituted by WKAH BMC (t/wB/CII rats). *P < 0.01.
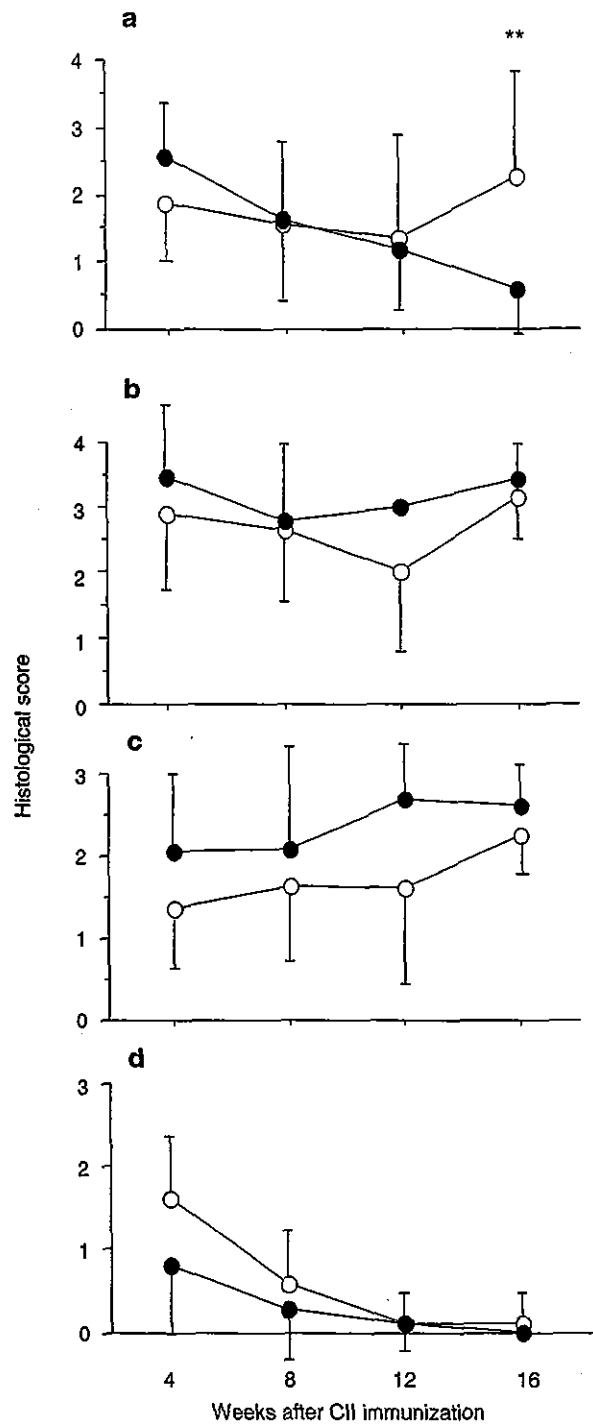
Figure 7 Histological score of arthritis. Infiltration of inflammatory cells (a), proliferation of stroma (b), fibrosis (c) and proliferation of synovial lining cells (d) were evaluated as indicated in Figure 1 and Table 1. At each time point, data from 10 ankles of five rats are shown. ●, w/tB/CII rats; O, t/wB/CII rats. **P < 0.05.

weeks after immunization: w/tB/CII, 10.52 ± 1.71 mm; t/wB/CII, 8.07 ± 1.04 mm; P = 0.001). However, the diameter of t/wB/CII joints started to increase further 12 weeks after immunization (Figure 6). Ultimately, the degree of joint swelling was equivalent to that seen in w/tB/CII rats (at 16 weeks after immunization: w/tB/CII, 11.52 ± 3.79 mm; t/wB/CII, 10.64 ± 1.85 mm; P = not significant). A histological exam-

ination revealed that a severe infiltration of inflammatory cells was evident in arthritic joints of w/tB/CII rats at 4 weeks after immunization, but the numbers of inflammatory cells accumulating at arthritic joints decreased time dependently in these rats (Figure 7a). On the contrary, inflammatory cell accumulation persisted in arthritic joints of t/wB/CII rats, although the degree was less than that of w/tB/CII rats at 4
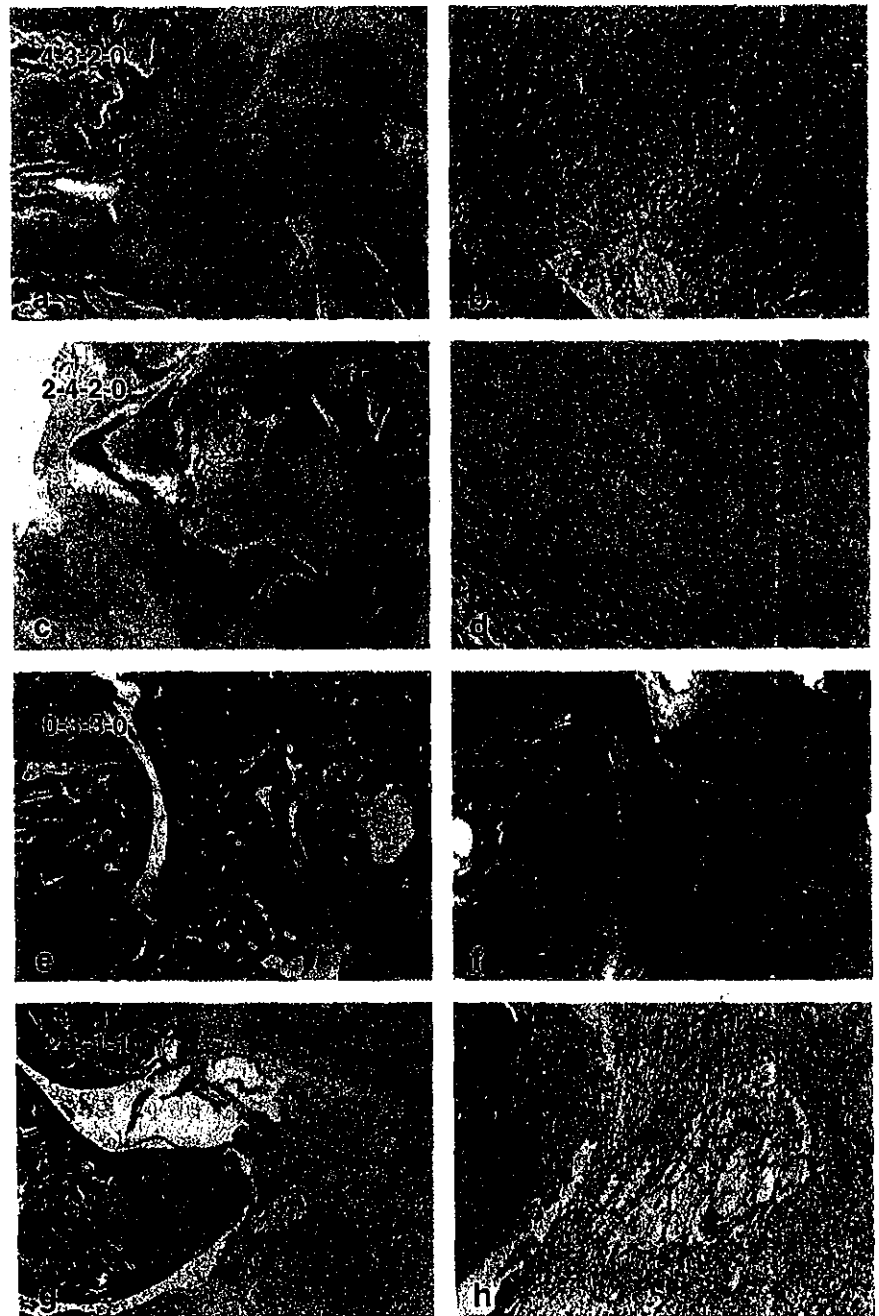
Figure 8 Representative photographs of arthritic joints of w/tB/CII (a, b, e, f) and t/wB/CII (c, d, g, h) rats at 4 (a–d) and 16 (e–h) weeks after type II collagen (CII) immunization. The right panels represent views of high-power field (original magnification, ×100) of the left panels (×20). The four numbers in the left panels, from left to right, represent histological scores for infiltration of inflammatory cells, proliferation of stroma, fibrosis and proliferation of synovial lining cells, respectively.